



Assessment of Novel Boron-doped Mesoporous Bioactive Glass Nanoparticles Loaded Alginate Hydrogel in Dogs

Marwa Samir Naga^{a,*}, Elbadawy Abdel Aziz Kamoun^{b,c,*},
Maha Abdel Moaty^a, Ahmed Zaki Ghareeb^d, Mona Mohy El Din^a,
Samia Soliman Abdel Rehim Omar^e

^a Dental Biomaterials Department, Faculty of Dentistry, Alexandria University, Alexandria, Egypt

^b Department of Chemistry, College of Science, King Faisal University, Al-Ahsa 31982, Saudi Arabia

^c Polymeric Materials Research Department, Advanced Technology and New Materials Research Institute (ATNMRI), City of Scientific Research and Technological Applications (SRTA-City), New Borg Al-Arab 21934, Alexandria, Egypt

^d Centre of Excellence for Drug Preclinical Studies (CE-DPS), Pharmaceutical and Fermentation Industry Development Centre, City of Scientific Research and Technological Applications, New Borg El Arab, Alexandria, Egypt

^e Oral Biology Department, Faculty of Dentistry, Alexandria University, Alexandria, Egypt

ARTICLE INFO

Article history:

Received 28 November 2024

Received in revised form

26 March 2025

Accepted 15 April 2025

Available online xxx

KEY WORDS:

Dentin regeneration

Boron

Vital pulp therapy

Mesoporous bioactive glass nanoparticles

Alginate hydrogel

Regenerative pulpotomy

ABSTRACT

Introduction: Dentin regeneration is pivotal to preserve tooth vitality. This study aims to evaluate, histologically, the dentine regenerative potential of a novel injectable boron-doped, mesoporous, bioactive glass nanoparticle (BMBGNPs) loaded alginate hydrogel in dogs

Methods: The formulation and optimisation of the novel alginate/BMBG NPs (20 wt. %) loaded composite hydrogel were performed. Next, 66 teeth of 3 dogs were allocated into 3 groups (each including 22 teeth) according to post-operative follow-up period: group I: 2 weeks, group II: 4 weeks, and group III: 8 weeks. Each group was further subdivided according to pulpotomy filling material into two subgroups, with subgroup 1 (alginate/BMBGNPs (20 wt. %) loaded hydrogel) and subgroup 2 mineral trioxide aggregate (MTA). Pulp chambers were mechanically exposed through class V cavities. A complete pulpotomy was executed. The tested materials were positioned on the radicular pulp and finally covered with resin composite restorations. One dog was sacrificed after 2, 4, and 8 weeks. Teeth were prepared for histological evaluation assessing inflammatory cell response, pulp tissue organisation, and dentin bridge formation. The Mann-Whitney U test was employed to evaluate the scores of histological parameters between tested materials ($P \leq .05$).

Results: Alginate/BMBG NPs (20 wt. %) loaded hydrogel showed normal pulp configuration at 2 and 4 weeks, which was enhanced after 8 weeks ($P \leq .05$). Moderate inflammatory reaction was noted at 2 weeks, which was improved after 4 and 8 weeks ($P \leq .05$). MTA group demonstrated less favourable pulpal response and inflammatory reaction with a statistically significant difference across all observational periods ($P \leq .05$). After 8 weeks all teeth in group 1 exhibited the thickest dentin bridge ($P \leq .05$).

Conclusions: Alginate/BMBG NPs (20 wt. %) loaded hydrogel offers the promise of regenerating dentin and maintaining pulp vitality reaching the desired level as an alternative to MTA.

Clinical Relevance: Alginate/BMBG NP loaded hydrogel is an alternative, reliable option for vital pulp therapy.

© 2025 The Authors. Published by Elsevier Inc. on behalf of FDI World Dental Federation.

This is an open access article under the CC BY-NC-ND license

(<http://creativecommons.org/licenses/by-nc-nd/4.0/>)

Introduction

Vital pulp therapies are biologically based minimally invasive concepts.¹ Their main target is to handle deep carious lesions while maintaining pulp vitality. Pulpotomy is a crucial

* Corresponding author. Faculty of Dentistry, Alexandria University, Alexandria, Egypt.

E-mail addresses: marwa.naga.dent@alexu.edu.eg (M.S. Naga), ekamoun@kfu.edu.sa (E.A.A. Kamoun).

<https://doi.org/10.1016/j.identj.2025.04.008>

0020-6539/© 2025 The Authors. Published by Elsevier Inc. on behalf of FDI World Dental Federation. This is an open access article under the CC BY-NC-ND license (<http://creativecommons.org/licenses/by-nc-nd/4.0/>)

therapeutic method for both deciduous and permanent teeth. Pulpotomies are straightforward, time saving, and relatively cheaper than pulpectomy or root canal therapy.² Different pulpotomy agents are applied including bio-dentine, bio-aggregate and mineral trioxide aggregate (MTA). None of them has been confirmed to be perfect.³ Accordingly, this was the driving point behind the exploration for a biocompatible biomaterial which meets all the needs desired to obtain a prosperous regenerative pulpotomy approach.³ Consequently, the scaffold-established tissue regeneration paradigm is considered a favourable procedure to restore destructed dentin/pulp complex.⁴

Soft scaffolds such as injectable hydrogels imitate extracellular matrix configuration and are important in dentin pulp complex regeneration. They work as a template for delivery of cells, bioactive molecules, and therapeutic agents, conveniently, to desired locations in a minimally invasive way.⁵ Hydrogels derived from natural polymers such as alginate, keratin, and collagen, among others, have superior advantages including being non-cytotoxic, biocompatible, low cost and obtainable.⁵ Alginate is an anionic polysaccharide originating from brown algae. Alginate hydrogel is biologically accepted, harmless, nonimmunogenic, and biodegradable. Also, alginate hydrogels act as a template to assist dental regeneration, and it has been demonstrated that they enhance the secretion of dentin matrix.⁶ Bioactive glass nanoparticles (BG-NPs) have been proposed for dentin regeneration due to their promising effects such as bioactivity, angiogenesis and antibacterial. Furthermore, BG-NPs bind to living tissues and potentiate new tissue growth and differentiation while dissolving over time.⁷

Lately, mesoporous BGs nanoparticles (MBG NPs) have been discussed. They are of higher specific surface area and have highly ordered pores and superior bioactivity than traditional BGs.⁸ MBG NPs improve tissue regenerative capacity.^{8,9} They contribute to odontogenic differentiation of SHEDs and dentin-like matrix mineralisation.¹⁰ Boron is an 'ultra trace element'.¹¹ Innovative applications in the dental field supported the addition of boron to dental materials because doing so produced favourable biological outcomes such as liberation of growth factors and cytokines and elevation of extracellular matrix development. Moreover, various physical properties of different dental biomaterials have been improved by the incorporation of boron. Boron affects different glass characteristic features, thus regulating cell-glass interaction *in vivo* and *in vitro*.¹² Boron-based bioactive glasses proved to be biocompatible and non-cytotoxic and to reinforce cell adhesion, growth, and differentiation.^{12,13} Although bioactive glass nanoparticles are well established for tissue regeneration, their regenerative potential as a pulpotomy filling material has not been extensively studied. To the best of the author's knowledge, few previous studies have evaluated the application of BG NPs to dental tissue engineering using human dental pulp stem cells (hDPSCs).¹⁴ Therefore, the conjunction of the above-noted biomaterials with a proper, optimal formulation and injection technique presents a biomimetic perspective appropriate for dental tissue regeneration. Consequently, this combines the preferences of each separate material and reduces their limitations to release their full regenerative potential. It could also promote the

development of an injectable *in situ* forming hydrogel, which could accurately reach every inaccessible point in the operating area. In addition, this could ascertain that all predecessors were sufficiently blended, and hydrogel characteristics were not negatively affected. Furthermore, it could allow effortless, even, and gentle discharge of a non-heterogeneous, steady, and coherent hydrogel form.¹⁵

Animal models are important to bridge the translational gap that exists between preclinical and clinical research. Therefore, the proper choice of a validated animal model is crucial to predict the clinical question. Dog as an animal model has been chosen as a very suitable experimental model (preclinical model) in the *in vivo* part of the study for the following reasons: (1) the formation and inducement mechanisms of dentin in dogs are like those in human beings, but the rate of reparative dentinogenesis is not the same; (2) pulp tissue in dog's teeth resembles that of humans; and (3) dogs have numerous teeth in every quadrant, which helps to compare various biomaterials in the same dog.¹⁶

Accordingly, the current study aims to prepare and determine the optimal criteria of a novel injectable alginate hydrogel, loaded with BMBG NPs (20 wt.%), as a promising pulpotomy filling material for dentin regeneration. It also aims to evaluate histologically its regenerative potential in pulpotted dogs' teeth through assessing inflammatory cell response, pulp tissue organisation and dentin bridge formation.

Materials and methods

Material Preparation

Sodium alginate powder, anhydrous calcium chloride powder, and ethanol were obtained from Sigma-Aldrich Chemie. Boron-doped mesoporous bioactive glass nanoparticles (44% SiO₂, 33% CaO, and 9% P₂O₅, 14% Boron [B₂O₃]) (NT-MBG 58S3.6 B14) were obtained from Nano Tech. White mineral trioxide aggregate (MTA) was acquired from Keeper's Dent. The glass ionomer composite liner was obtained from PROMED-ICA. Resin composite restoration and adhesive bond were both supplied by 3M ESPE.

A. Determination of the optimum criteria of novel injectable boron-doped mesoporous bioactive glass nanoparticles (BMBG NPs) loaded sodium alginate composite hydrogel.

Fabrication of injectable sodium alginate hydrogel

For establishing the optimal standards for constructing an injectable sodium alginate hydrogel, the ideal condition was achieved at 7 wt.% sodium alginate, and 20 wt.% anhydrous calcium chloride was selected. This showed the best setting time at 15 minutes, injectability (easy/moderate), pH measurement, viscosity behaviour, swelling ratio percentage at predetermined time periods, and hydrolytic degradation (weight loss %).¹⁵

Generally, a 7 wt.% aqueous sodium alginate phase was achieved by dissolving the sodium alginate powder homogeneously in sterile distilled water (Milli-Q IQ7000 ultrapure

water system, Merck) in a clean environment, employing a magnetic stirrer (F91T, FALC) until a fully unobscured cloudless solution was achieved. A sterile syringe filter was used to filter the obtained solution. Next, anhydrous calcium chloride powder was dissolved in sterile distilled water (Milli-Q IQ7000 ultrapure water system, Merck) to achieve the mineral phase (20 wt.% anhydrous calcium chloride). Lastly, both phases were loaded into separate chambers of a specially set up sterile dual-syringe assembly for mixing and injection, creating a discharge of a consistent formulation¹⁵ (Figure S1, supplementary data).

Construction of injectable boron-doped mesoporous bioactive glass nanoparticles (BMBG NPs) loaded sodium alginate composite hydrogel

Sodium alginate hydrogel with BMBG NPs (20 wt.%) was prepared following the above-mentioned procedure¹⁵ as illustrated in Figure S2 and Table S1 (supplementary data).

B. In vivo histological animal study: Histological evaluation of injectable alginate hydrogel loaded with boron-doped mesoporous bioactive glass nanoparticles (BMBG NPs) (20 wt. %) in pulpotomised dogs' teeth

The current *in vivo* study assessed histologically, in pulpotomised dog's teeth, the execution of the novel injectable alginate/boron-doped mesoporous bioactive glass nanoparticles (20 wt.%) loaded composite hydrogel that has achieved the most favourable physicochemical performance in our previous research work¹⁵ through analysing the inflammatory cell response, pulp tissue organisation and the reparative dentin bridge.

Study design and sample size calculation

The present work was a histological split mouth-controlled animal study. A total of 66 permanent teeth of 3 healthy adult male mongrel dogs were used. The sample size was estimated to be 10 teeth for every group, raised to 11 to compensate for operating and methodological errors. Sample size calculation was settled on comparison of means, supposing alpha error = 5% and study power = 80%, and decided or resolved by GPower 3.1.9.4 sample size calculator software (<https://www.psychologie.hhu.de/arbeitsgruppen/allgemeine-psychologie-und-arbeitspsychologie/gpower>).^{17,18} Any animal removed from the study was replaced to conserve the sample size. This animal number was calculated based on precise calculations accomplished in the Department of Medical Statistics and the Medical Research Institute, Alexandria University.

Animals

The present work was approved by the institutional ethics committee, Faculty of Dentistry, Alexandria University (IRB No. 00010556-IORG No. 0008839) (0240-April 2021). The authors adhered to all institutional and international guidelines for

animal care and use throughout the current study. All animal research reporting *in vivo* experiments guidelines (ARRIVE) were also considered. Three adult male mongrel dogs with an approximate weight of 15-20 kg and aged 1-2 years were chosen for the current study (Table S2, supplementary data). Animals were acquired from the Animal House of the Medical Research Institute, Alexandria University. Dogs were examined, vaccinated and kept under supervision in different cages (1.5 m × 2.5 m × 3 m). They were accommodated under the exact suitable circumstances of breathing, diet, care, and 12-hour light/dark pattern and were served soft-diet meals and clean water every day. The principal diet regime was reviewed and, if necessary, adjusted daily throughout the observation period.¹⁹ The study was conducted in the City of Scientific Research and Technological Applications, New Borg El-Arab City, Alexandria, Egypt.

Classification of samples, randomisation, and allocation concealment

A total of 66 permanent teeth were included in this study. The maxillary and mandibular, right and left permanent molars, premolars, canines, and incisors were used in each quadrant. The selected teeth were divided based on the postoperative follow-up period into 3 major groups (22 teeth each): group I—2 weeks, group II—4 weeks, and group III—8 weeks. Each group was further subdivided based on the pulpotomy filling material into two equal subgroups (11 permanent teeth each), providing a total of 22 teeth in each dog, with subgroup 1 (alginate/BMBGNPs (20 wt.%) loaded hydrogel) and subgroup 2 (MTA) as the control. Dogs were randomly assigned using computer-generated random numbers to 1 of the 2 groups based on the type of pulpotomy filling material used.^{20,21} The allocation sequence/code was concealed from the individual allocating the samples to the intervention arms using a sealed opaque envelope.²²

Pulpotomy procedure

All operations were carried out in a clean, sterilised room. After fasting the dogs for 12 hours, general anaesthesia was promoted by an S/C injection of 0.05 mg/kg atropine sulphate (atropine sulphate 1% R; ADWIA), IM injection of 1 mg/kg xylazine HCL (Xylaject 2% R; ADWIA), and IM injection of 10 mg/kg ketamine HCL (Keiran R; EIMC Pharmaceuticals Co.). Anaesthesia was sustained with gradual doses of thiopental sodium 2.5% solution (Thiopental sodium R; EIPICO) at a dose of 25 mg/kg supplied intravenously.²⁰ Oral cavity was cleaned with 0.2% chlorhexidine gluconate (JK Dental, A.R.E), and a rubber dam was positioned carefully. Then pulp chambers were mechanically exposed through class V cavities at the buccal surface of chosen teeth, 0.5-1 mm above the gingival margin, using an inverted cone carbide bur (Komet, Lemgo, Germany) at a low speed and under adequate saline irrigation. The coronal portion of the pulp was extirpated with a sharp endodontic excavator (DG16, Dental USA). Haemostasis was achieved after employing adequate pressure with sterile cotton pellets and copious irrigation with sterile

saline solution (El Fath For Drug And Cosmetics Industry [FICO]).²³ All tested materials were carefully positioned on top of the persisting radicular pulp tissue, filling up the pulp chamber. In subgroups I1, II1, and III1, freshly provided sterile alginate/BMBGNPs loaded hydrogel was injected inside the pulp chamber. In subgroups I2, II2, and III2, white MTA was administered according to manufacturer's recommendations. Any remnants of materials were eliminated by moist cotton pellets. Then, once the tested materials began to set, all cavities in the operated teeth were covered with a thin layer of glass ionomer cement. Next, resin composite restorations were incrementally placed and light-cured.²⁴ All steps were done by 1 skilled operator. After the intervention, all animals were supervised every day to evaluate the presence or absence of any infection. Animals continued a soft diet and were given analgesia with ibuprofen (Argipronex, Medizen pharmaceutical industries) (10 mg/kg every 8 hours for 24 hours after intervention).

Histological examination

One dog was sacrificed after 2, 4, and 8 weeks, each using an intravenous excess-dose injection of concentrated thiopental sodium (EPICO pharmaceutical industry) (20 mL of 5% thiopental sodium). Jaw segments encompassing manipulated teeth and sections of surrounding soft tissue were resected out of the jaws (maxilla and mandible). Bone segments, including the operated teeth, were excised and prepared for histological evaluation.¹⁹ Teeth were fixed in 10% neutral buffered formalin (Research-Lab Fine Chem Industries) for 1 week. Specimen decalcification was accomplished using 10% trichloroacetic acid (Advent Chembio Pvt), which lasted for about 2 months. After decalcification, specimens were dehydrated in ascending concentrations of ethanol (Piochem Laboratory chemicals store) and cleared in xylene (EMSURE ACS, ISO, Reag. Ph Eur Xylene (isomeric mixture), Sigma Aldrich Company, Merck KGaA), embedded in paraffin wax (Hista-Flex, Hurst Scientific), after which they were mounted in paraffin blocks. Paraffin-infiltrated teeth were successively sectioned in a vertical, mesiodistal direction through the capping location and the pulp to obtain sections of 5- μ m thickness. Serial sections that included the deepest part of the cavity and the pulp tissue below were selected.¹⁶ These sections were stained using hematoxylin and eosine (H&E) stain (Sigma-Aldrich Company, Merck Chemicals KGaA). Two blinded qualified and practised examiners assessed the specimens using coded samples all through the research work to prevent any probable bias. Ultimately, sections were evaluated using a light microscope linked to a high-resolution camera (Optikam C-B5 Digital Camera) to assess the inflammatory cell response, pulp tissue organisation and reparative dentin bridge formation according to the following scoring system represented in (Table S4, supplementary data).²⁵

Statistical analysis

The Mann-Whitney *U* test was employed to evaluate the scores of histological parameters between the 2 materials.

Meanwhile, the Kruskal-Wallis test, followed by Dunn's post hoc test with Bonferroni correction in case of significant results, was used to examine variations in these scores across different time intervals. All tests were 2-tailed, and the significance level was set at $P \leq .05$. Data were assessed using IBM SPSS, version 23 of Windows.

Results

Histological results

Alginate/BMBG NPs loaded hydrogel (subgroup 1)

After 2 weeks. Normal appearance of the pulp tissue prevailed in most of the sections (score 1 [72.7%]) with a moderate inflammatory reaction (score 2 [72.7%]) (Figures S3 and S4 and Tables S5 and S6, supplementary data). Inflammatory cells were traced adjacent to slightly disorganised odontoblast cells with few scattered inflammatory cells among the central tissues adjacent to dilated blood vessels (Figure S5A-D, supplementary data). Some figures of the hydrogel were traced among the pulp tissue in many sections with preservation of pulp structure (Figure S5E, supplementary data). Small bridges ranging from mild to moderate thickness were seen (score 1 (18.2) and score 2 [81.8] [%], respectively) (Figure S6 and Tables S5 and S6, supplementary data) and most of them exhibited frank attachment to the dentin walls of the roots (Figures S5A and S7A-C, supplementary data). In 1 of the formed bridges, the fibrodentin (FD) structure was seen. It mingled with the applied hydrogel pulpotomy material (Figure S7D, supplementary data). Another bridge exhibited a fibro-cellular structure like osteodentin (OD) (Figure S7E, supplementary data), while a different bridge consisted of a combination of both FD and OD structures was also displayed (Figure S7F, supplementary data). An important observation was encountered in high-power views of those bridges, which revealed accommodation of dentin-like tissue inside the pores of the hydrogel (Hg) (Figure S7G and H, supplementary data) with an obvious appearance of released boron nanoparticles (B) inside the pores (Figure S7I, supplementary data).

After 4 weeks. Normal pulp organisation was observed particularly in the central region with a slightly disorganised odontoblast layer (score 1 [54.5%]). Mild inflammatory reactions prevailed adjacent to odontoblasts (score 1 [81.8%]), which was accompanied by a profound blood supply (Figures 1A, D and 2B, C, Figures S3 and S4, and Tables S5 and S6, supplementary data). Different configurations of the formed bridges in different teeth were noted, but generally they were all thicker (moderate thickness) (score 2 [90.9%]) than those of the 2-week observation period (Figures 2A, D and G, Figure S6, and Tables S5 and S6, supplementary data). One of these bridges appeared homogenous and exhibited a tubular configuration with fine dentinal tubule-like structures extending across its full thickness. Odontoblast-like cells were traced on the apical border of the newly formed tubular dentin bridge. A slight incorporation of the hydrogel into the superficial part of the newly formed dentin bridge structure was clear (Figure 2A and B). Regenerated dentin (rd) was

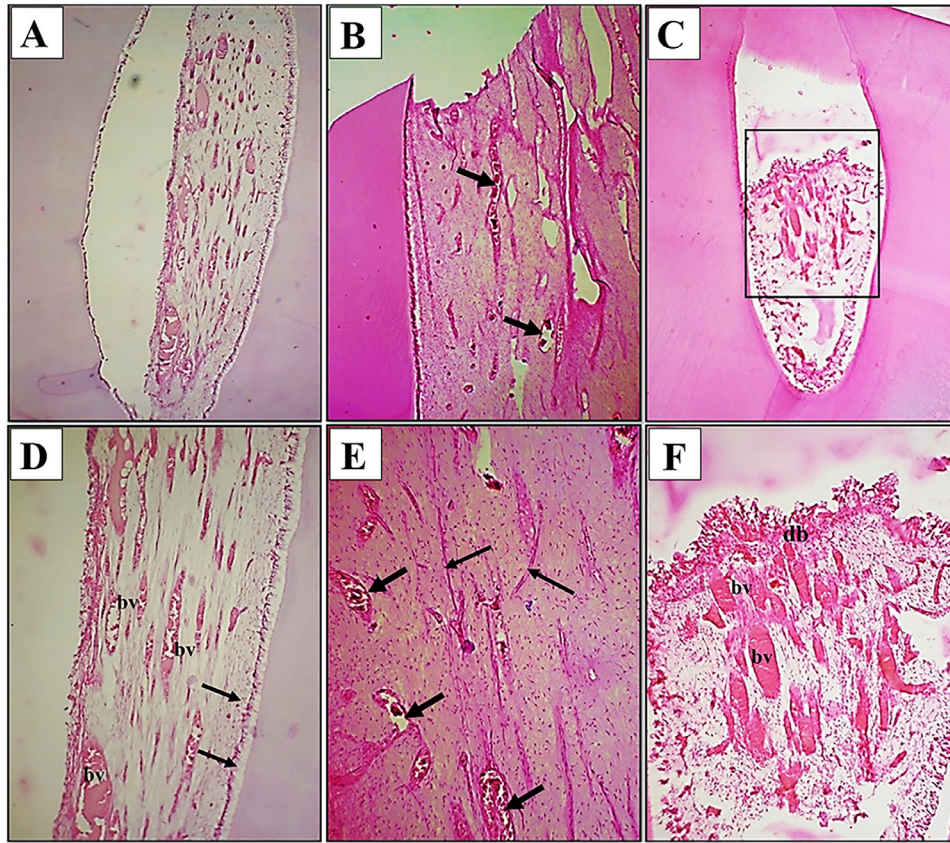


Figure 1 – Decalcified sections (DSs), H&E, pulp reaction in subgroup II1 (alginate/BMBG NPs loaded hydrogel) (A and D) and subgroup II2 (MTA) (B, C, E and F) (4 weeks). D is a higher magnification of A. E and F are higher magnifications of B and C, respectively. In A and D normal pulp organisation is seen with mild inflammatory reaction, slightly disorganised odontoblasts (arrows) and profound blood supply (bv). In B and E (MTA group) normal pulp organisation is evident with moderate inflammatory reaction, normal pulp vascularity (thick arrows) and neural distribution (thin arrows). In C and F severe inflammatory reaction is seen adjacent to the formed dentin bridge (db) with disorganisation of odontoblasts (inset) and vertically arranged blood vessels (bv) towards the bridge. Magnification: A and B—x100, C—x40, D–F—x400.

observed lining both sides of the root canal (Figure 2A, B, D, H). Another section showed a newly formed bridge of moderate thickness and a well-organised pattern of dense collagen fibres (Figure 2D–F). An outstanding collaborating phenomenon was seen where the hydrogel intermingled with the formed dentin-like tissue bridge (Figure 2D–F, H and Figure S8A and B, supplementary data). In this situation, it seemed that the hydrogel constituted parts of the formed bridge; even the brownish colour of boron particles was clearly distinguished among the dentin bridge (db) and the hydrogel (Figure S8A and B, supplementary data). One of the formed bridges appeared ectopic in location. This ectopic dentin bridge (edb) was of moderate thickness, homogenous, and showed a tubular structure (Figure 2D and G).

After 8 weeks. The pulp exhibited mild (low-grade) inflammation (score 1 [100%]) (Figure S3 and Tables S5 and S6, supplementary data). Odontoblasts appeared well organised in most of the examined sections (Figure 3A), although in 1 of the sections they appeared slightly disorganised (Figure 3D).

Thin streaks of the hydrogel could be traced bounding the pulp at a distance from the formed bridge, and traces of this hydrogel were seen even in the pulp tissue, especially bordering the small and large blood vessels (Figure 3B, C, E, F). In all the examined sections, normal organisation of the pulp tissue components was a predominating feature (score 3 [81.8%]) and included angiogenic figures and neural elements (Figure 3A and D, Figure S4, and Tables S5 and S6, supplementary data). An outstanding thickness of the formed bridges was a prevailing finding (score 3 [100%]) (Figure 4A, Figure S6 and Tables S5 and S6, supplementary data). The structure of the formed bridge included OD in the most superficial layer which contained fine particles of the hydrogel. The trapped cells could be clearly traced among the bulk of OD (Figures 4B and C). The deeper layer consisted of tubular dentin-like tissue (TD) with a layering pattern and dark lines in between the layers like the incremental lines of von Ebner and exhibited an outline parallel to that of the pulp contour (Figure 4B and C). Regenerated dentin (rd) formation was seen on both sides of the root canal with evident dentinal tubule-like structures extending along its full

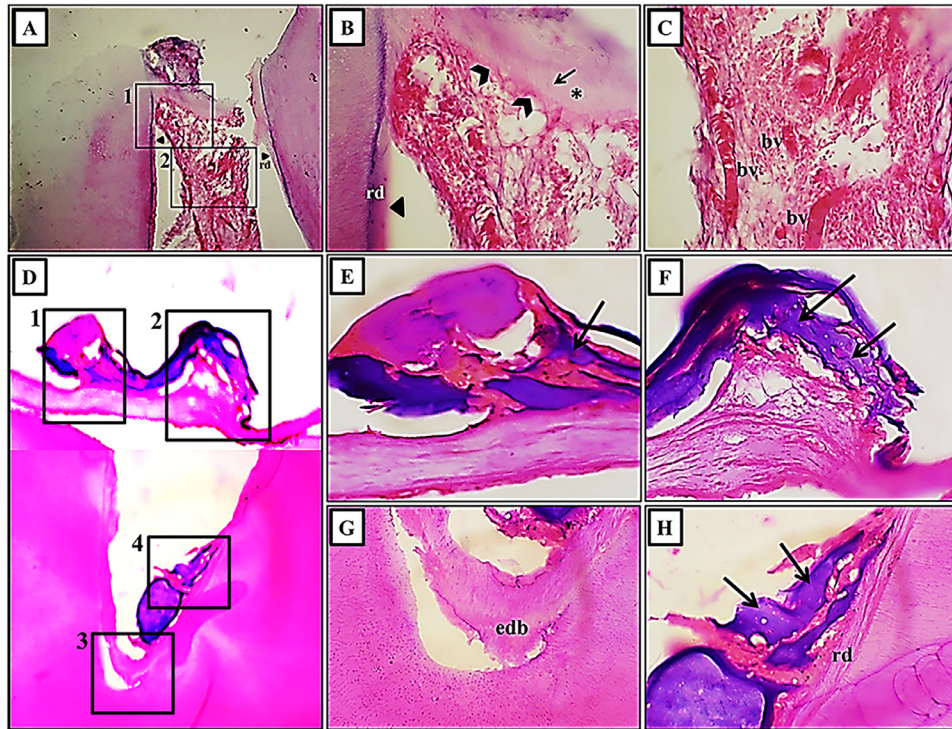


Figure 2 – Decalcified sections (DSs), H&E, subgroup II1 (alginate/BMBG NPs loaded hydrogel) (4 weeks). Moderate thickness of the formed bridges is showing in A and D. B is a higher magnification of inset 1 in A. C is a higher magnification of inset 2 in A. E and F are higher magnifications of insets 1 and 2 in D, respectively. G and H are higher magnifications of insets 3 and 4 in D, respectively. D is a compound figure. In B a homogenous structure of the formed bridge (asterisk) is seen exhibiting tubular dentin-like structure (arrow) and odontoblast-like cells (chevrons) arranged on the apical border of the bridge. In A and B regenerated dentin (rd) (arrowhead) is seen on both sides of the root canal and merging with the main body of the formed bridge. In C mild pulpal inflammation and profound blood supply (bv) are revealed. In D-F note the well-organised dentin formed bridge (moderate thickness) with evident dense organised collagen fibres. In D-F and H incorporation of the hydrogel into the formed bridges is seen (insets 1, 2, 4 and arrows). D and G show ectopic dentin bridge (edb) formation at the apical part of the root canal (inset 3) and its merging with rd along the adjacent canal wall. Magnification: A and D (compound figure) —x100; B, C, E-H—x400.

thickness with apparent incremental lines. This rd appeared confluent with the bulk of the formed bridge (Figure 4A and D).

MTA group (subgroup 2) (control group)

After 2 weeks. Moderate inflammatory reaction (score 2 [54.5%]) was seen in most of the obtained sections in this group with disorganised odontoblasts and few figures of oedema in association with a lymphatic system (score 1 [72.7%]) (Figures S3, S4, and S9 and Tables S5 and S6, supplementary data). In 1 of the sections, disorganised aggregations of pulp tissue were seen adjacent to the formed bridge. This aggregated pulp tissue contained a high density of inflammatory cells (Figure 5A and D). Thin (mild) dentin bridges (score 1 [54.5%]) of either FD (Figures 5A-D) or a combination of FD and OD (Figure 5E and F) were noted with focal areas of attachment to the dentin walls of the pulp canal (Figure 5A, C, E, F) (Figure S6 and Tables S5 and S6, supplementary data).

After 4 weeks. Normal pulp tissue was seen (score 1 [81.8%]), although moderate inflammatory reactions among the tissues of the pulp persisted (score 2 [63.6%]) (Figures S3 and S4 and Tables S5 and S6, supplementary data). Well-organised odontoblast cells were traced with normal pulp vascularity and neural distribution (Figure 1B and E). But in some sections the inflammatory reaction was severely accentuated adjacent to the site of the bridge, with disorganisation of the odontoblast layer all over the pulp boundary. The blood vessels (bvs) were seen arranged in a vertical direction towards the site of the bridge (Figure 1C and F). Moderate bridge thickness was noted with structural disorganisation (score 2 [63.6%]) (Figure 6A and D, Figure S6, and Tables S5 and S6, supplementary data). At a high power of examination, the bridge structure included many distinct layers comprising either FD (Figure 6B and C) or a combination of FD and OD (Figure 6E and F).

After 8 weeks. The pulp exhibited a moderate inflammatory reaction (score 2 [45.5%]) with slight disorganisation of the odontoblast cells and marked vascularisation (score 1 [72.7%])

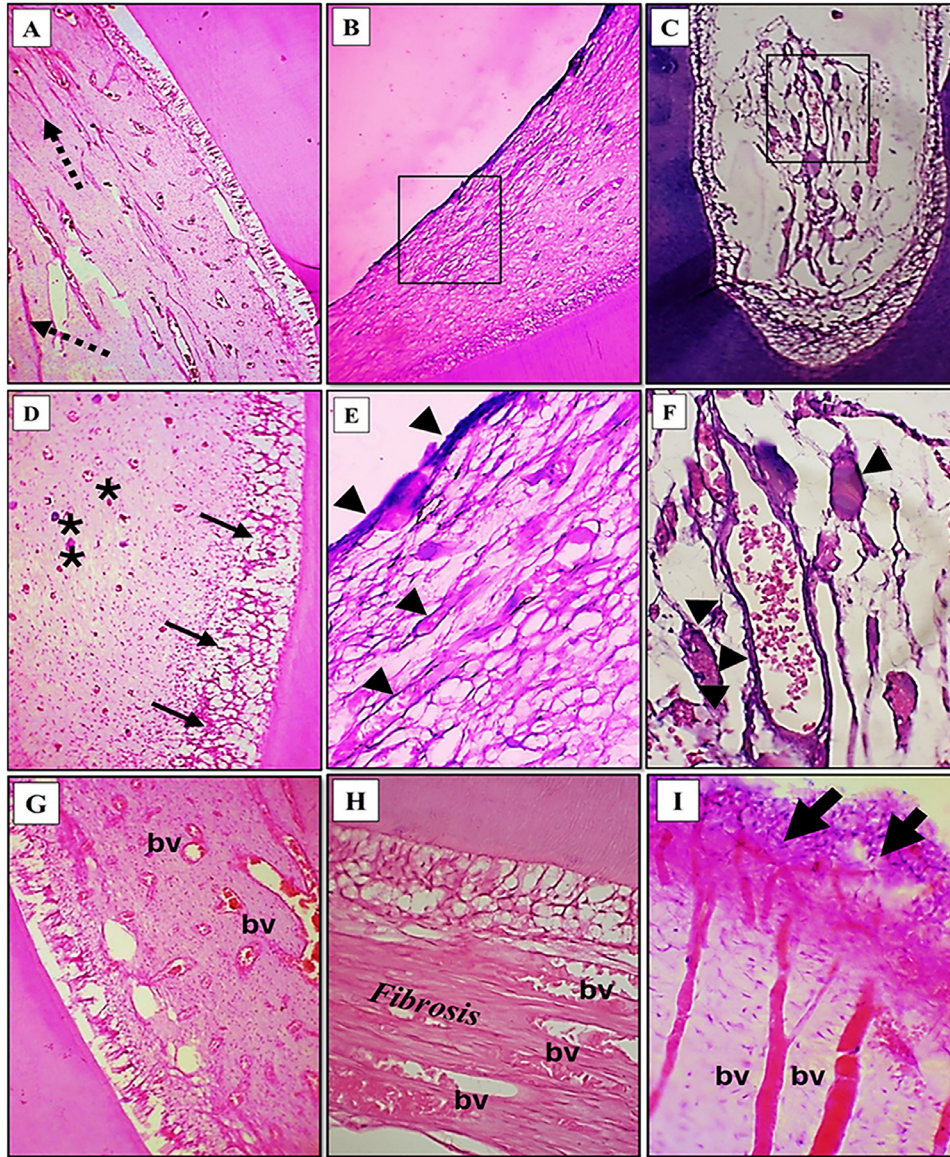


Figure 3 – Decalcified sections (DSs), H&E, pulp reaction in subgroup III1 (alginate/BMBG NPs loaded hydrogel) (A-F) and subgroup III2 (MTA) (G-I), (8 weeks). E and F are higher magnifications of the boxed areas in B and C, respectively. In A mild inflammatory reaction is seen with well-organised odontoblasts and evident neural elements (dotted arrows). In B and E thin streaks (arrow heads) of the hydrogel are seen bounding the pulp at distance from the formed bridge. In C and F traces of hydrogel are observed among the pulp tissue and bordering small and large blood vessels (arrowheads). In D slightly disorganised odontoblasts (thin arrows) and angiogenic figures (asterisks) are seen. In G (MTA group) moderate inflammatory pulp reaction is seen with slight disorganisation of odontoblasts and profound vascularisation (bv). In H marked fibrosis of the pulp tissue adjacent to the odontoblasts is evident. In I complete disorganisation of odontoblasts (thick arrows) is seen adjacent to large blood vessels engorged with blood (bv). Magnification: A-C and G—x100; D-F and H and I—x400.

(Figure 3G, Figures S3 and S4, and Tables S5 and S6, supplementary data). In sections obtained from 1 of the specimens, the pulp exhibited complete disorganisation with frank fibrosis and disorganised odontoblasts (Figure 3H). Other sections showed complete disorganisation of odontoblasts adjacent to large blood vessels engorged with blood (score 2 [27.3%]) (Figure 3I). The formed bridge displayed variation in thickness and organisation with predominant moderate thickness (score 2 (81.8%)) and loss of homogeneous structure

in all parts (Figure S6 and Tables S5 and S6, supplementary data). Definitive loss of complete attachment to the dentin walls was noted (Figures 7A, B, C, and E). In 1 of the specimens, the definitive bridge consisted of tubular dentin-like tissue and was bordered from the pulp side by a thin layer of pre-dentin-like tissue and adjacent disorganised odontoblast-like cells (Figure 7C). In this specimen, the pulp revealed complete disorganisation, and many small vacuoles appeared between the central tissues

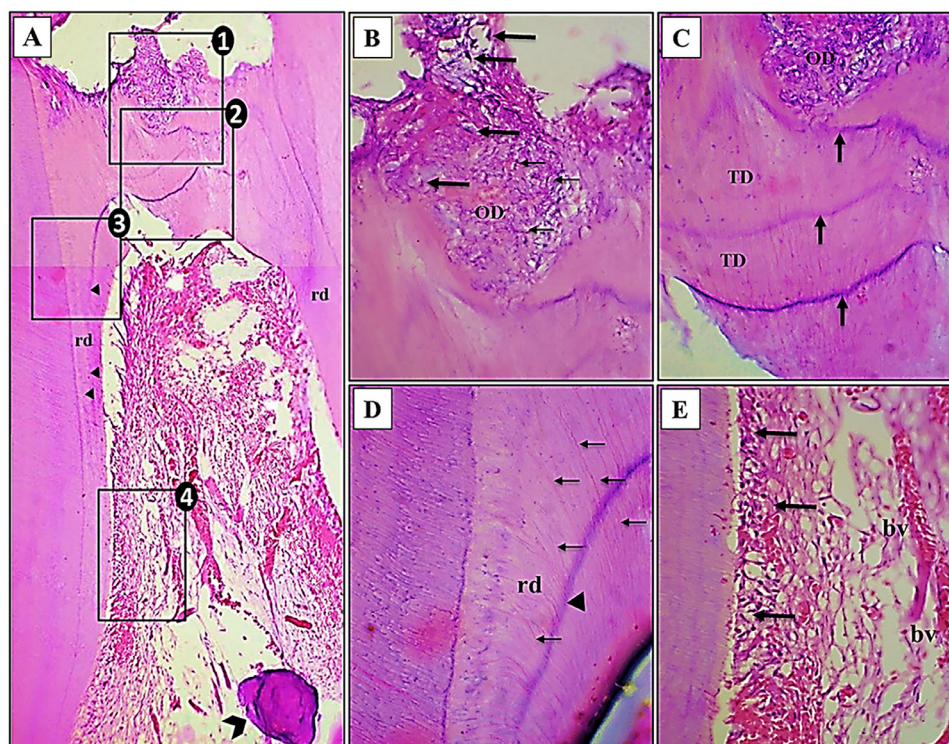


Figure 4—Decalcified sections (DSs), H&E, subgroup III1 (alginate/BMBG NPs loaded hydrogel) (8 weeks). **A** is a compound figure showing the outstanding thickness of a formed bridge including 3 distinct regions (insets 1, 2, 3). **B–E** are higher magnifications of insets 1–4 in **A**, respectively. In **A** note the false pulp stone deeper to the formed bridge (chevron). **B** is revealing osteodentin (OD) formation with trapped cells (thick arrows) and few particles of the hydrogel (thin arrows). **C** reveals formation of tubular dentin-like tissue (TD) exhibiting a layering pattern with evident von Ebner-like lines between the formed layers (arrows). In **A** and **D** regenerated dentin (rd) formation is seen on both sides of the root canal with evident dentinal tubule-like structures (thin arrows) extending along its full thickness with apparent incremental lines (arrow heads). This rd appears confluent with the bulk of the formed bridge. In **E**, a well-organised pulp structure is seen with organised odontoblasts (arrows) and profound blood supply (bv). Magnification: **A**— $\times 100$; **B–E**— $\times 400$.

and adjacent to the odontoblasts (Figure 7C and D). In both specimens MTA particles were traced in the formed bridges (Figure 7A, B, C, and E), inside the native dentin (Figure 7B and E) and in adjacent pulp tissue (Figure 7A, B, C, and E).

Discussion

The present experimental animal study was executed to evaluate, histologically, using pulpotomised dog's teeth, the performance of the novel nanoparticle-polymer based hydrogel in improving inflammatory cell response, preserving normal pulp tissue architecture and stimulating reparative dentin bridge formation. Based on the favourable physicochemical performance of alginate/BMBG NPs loaded hydrogel that was confirmed in our previous work,¹⁵ BMBG NPs (20 wt.%) was suggested as an optimal loading concentration to alginate matrix (Figure S10, supplementary data).

Complete pulpotomy was selected in the current study because it has been proven that coronal pulp tissue often includes microorganisms and discloses proof of inflammation and degenerative changes. Therefore, the affected part

of pulp tissue should be extirpated so regeneration would be allowed to develop at the entry of the pulp canal.²⁶ Consequently, applying a medicament directly on top of exposed pulp tissue is an advocated method, which allows pulp healing and reparative dentin regeneration.²⁷

Histological examination is the best method of choice that can provide objective data. For this reason, in the present study, the histological investigation aimed to judge outcomes at 2 weeks, 4 weeks, and 8 weeks. In line with different researches, the 2-week observation period was selected because it has been proven that at least 2 weeks are needed for the start of odontoblast-like cells differentiation and dentin bridge formation,²⁸ while no dentin bridge was traced prior to 2 weeks. Secondly, the 4- and 8-week follow-up periods were selected to observe pulp tissue organisation, resolution of inflammation and reparative dentin bridge formation.^{28,29}

Evidently, the novel alginate/BMBG NPs (20 wt.%) loaded hydrogel (subgroup 1) showed moderate inflammation after 2 weeks. Normal pulp tissue configuration and a notable improvement in inflammatory cell response prevailed after 8 weeks with statistical significance ($P \leq .05$). (Figures 1A and D, 2A–C, 3A–F, and 4E; Figures S3, S4, and S5A–E; and Tables S5 and S6, supplementary data).

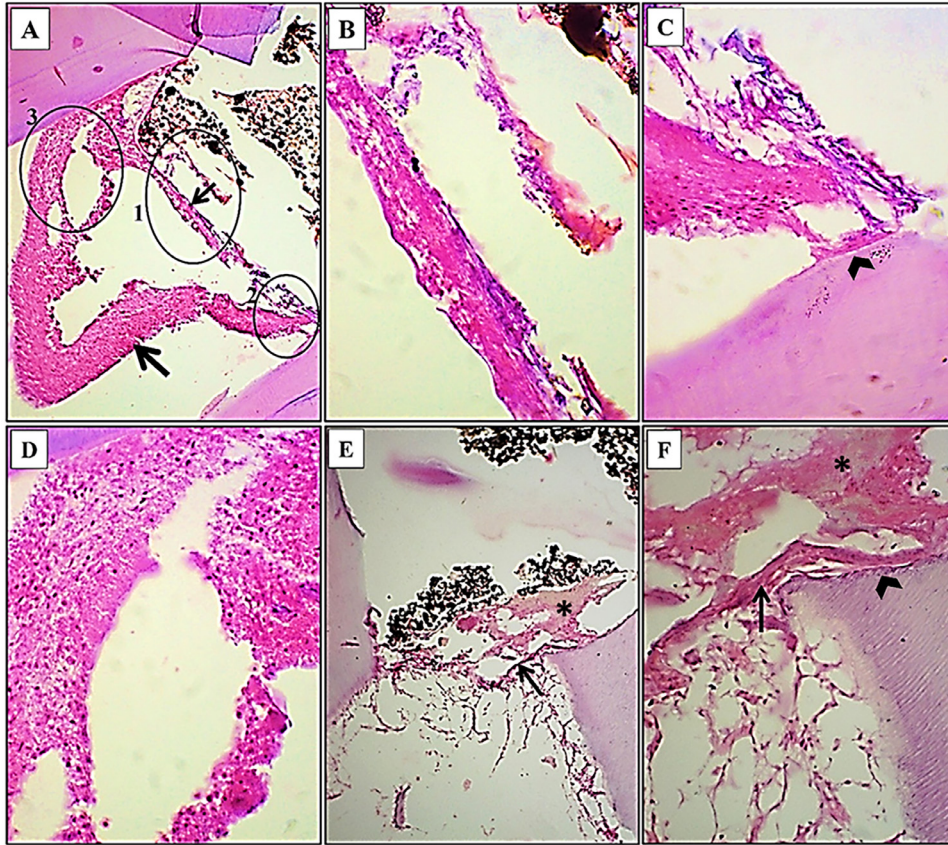


Figure 5 – Decalcified sections (DSs), H&E, subgroup I2 (MTA) (2 weeks). B, C and D are higher magnifications of circles 1, 2 and 3 in A, respectively. F is a higher magnification of the encircled area in E. In A and B formation of thin (mild) bridges of fibro-dentin (thin arrows) is seen. In E and F a combination of osteodentin (asterisk) and fibro-dentin (thin arrows) is noted. In A, C and D disorganised aggregation of pulp tissue (thick arrow) is clear adjacent to the formed bridge accommodating a high density of inflammatory cells. In A, C, E and F note the focal attachment of the formed bridges to the dentin walls of the roots. Magnification: A and E—x100; B, C, D and F—x400.

Presumably, this early, temporary inflammatory reaction might be a normal biological defensive reaction from the dental pulp to the pulpotomy procedure and the applied novel hydrogel.³⁰ Moreover, it could be probably due to the initial rapid ion release rate from the applied alginate/BMBG NPs loaded hydrogel. This quick ion release might sharply elevate the pH that is stabilised later on.^{30,31} Furthermore, this might be caused by the crucial action of the calcium phosphate wear remnants liberated from the deposited carbonated hydroxyapatite layer (bone-like layer). These wear remnants proved to be a powerful stimulus for the liberation of different pro-inflammatory cytokines when phagocytosed.³²

Various features of our novel hydrogel might contribute to the development of this ideal microenvironment. First, the antimicrobial behaviour of BG might play an eminent role. This behaviour was mainly due to high, consistent pH brought by BG that was acquired through different ways such as the liberation of silicon ion that is responsible for *in situ* pH increase, collagen production and angiogenesis.³³ Moreover, the great B_2O_3 amount that raised the pH value within a limited time and remained stable; nevertheless, the ultimate pH of borate glass (9.6) was lesser than silicate glass (11.5). This is attributed to the more powerful acidic character of $B(OH)_3$

compared to $Si(OH)_2$.³⁴ Also, boron has strong antibacterial activity.³⁵ Additionally, calcium ions and other alkalis liberated from BG could disrupt the cell membrane of bacteria.³⁵ Moreover, the nano-topography of BG improved its solubility and consequently increased the instant liberation of alkaline ions.³⁶ This could create a fine necrotic layer that might shield the underlying vital pulp and enhance the regenerative potential of adjacent pulp cells. Basically, high alkalinity tends to generate the regulatory IL-10 and denature pro-inflammatory cytokines; all have an anti-inflammatory influence.³⁷ Second, close marginal adaptation is another key factor which might stop microbial ingress and limit inflammatory process. This characteristic feature could be derived by the nano-sized BMBG particles with a large surface area,³⁸ hydrogel nature and the application technique used to fill the exposure site which probably ensured adequate delivery of hydrogel to inaccessible areas. This creates a tight seal minimising micro-leakage. Additionally, the carbonated hydroxyapatite layer (HCA) precipitated on the hydrogel surface could result in maintaining adequate marginal integrity.³⁹ Third, boron has anti-inflammatory⁴⁰ and angiogenic actions through elevating angiogenic gene expression¹² (Figures S10 and S11, supplementary data).

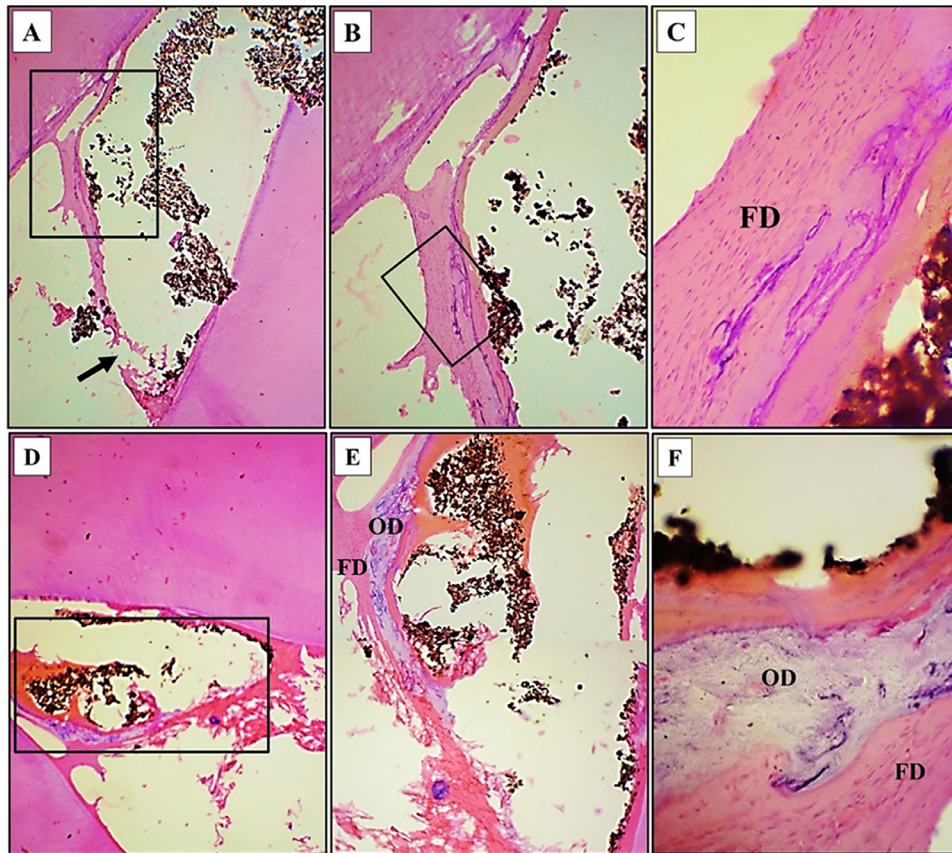


Figure 6 – Decalcified sections (DSs), H&E, subgroup II2 (MTA) (4 weeks). A and D showing different bridges of moderate thickness, structural disorganisation and discontinuation (arrow). B and C are higher magnifications of the boxed areas in A and B, respectively, showing the fibro dentin structure (FD) of the formed bridge. E is a higher magnification of the inset in D revealing the combined osteodentin (OD) and fibro dentin (FD) structure of another formed bridge. F shows a high-power view of OD and FD formation in another bridge of the same group, cellular inclusions are clearly seen in OD. Magnification: A and D –x40; B and E –x100; C and F –x400.

Current outcomes are in agreement with Arafa et al.,⁴¹ who showed that the addition of bioactive glass nanoparticles to resin composite and its adhesive had a promising pulp tissue response and inflammatory reaction after direct pulp capping in dogs.⁴¹

A striking picture was noted in some sections of the alginate/BMBG NPs (20 wt.%) loaded hydrogel group at the 8-week observation period showing thin hydrogel streaks bounding the pulp away from the created dentin bridge. Also, these hydrogel streaks were bordering the small and large blood vessels while pulp tissue was still displaying normal morphology with signs of new vascular ingrowth and neural elements. Accordingly, this could be considered as a positive sign of the novel hydrogel safe biocompatibility.

On the other hand, MTA (subgroup 2) demonstrated a less favourable pulpal response and an inflammatory reaction compared to the hydrogel group with a statistically significant difference across all observation time intervals ($P \leq .05$) (Figures 1B, C, E, F, 3G-I, and 5-7; Figures S3, S4, and S9; and Tables S5 and S6, supplementary data).

These results were consonant with the findings of a clinical histological study which demonstrated that retro MTA displayed the worst outcomes following direct pulp capping

as regards pulp tissue organisation, structure and dentin bridge thickness in comparison to Pro Root MTA.⁴²

Probably, this could be attributed to many reasons. First, MTA has an unsatisfactory sealing capability and marginal adaptation prior to reaching a complete set.⁴³ Second, its restricted antimicrobial behaviour might not prevent bacterial invasion towards pulp tissue.⁴⁴ Third, despite set MTA proving to be biocompatible and non-cytotoxic, few studies reported that MTA displayed great cytotoxicity when freshly prepared prior to setting. This was related to the high calcium dissolution from MTA which strongly raised the pH.⁴⁵ Fourth, MTA constituted toxic heavy metals contents (arsenic, chromium and lead) greater than the secure border determined by ISO 9917-1 (2007) that could hinder its biocompatibility.⁴⁶

Concerning reparative dentin bridge formation, basically all study groups demonstrated newly formed dentin bridges, and most of them were located opposite to the exposed pulp.

Virtually, after 2 weeks, the newly formed dentin bridges in the novel hydrogel group (subgroup I1) revealed various forms categorised as fibro dentin (FD), osteodentin (OD) or a combination of both. Generally, all of them were of mild to moderate thickness, continuous, traversed the summits of

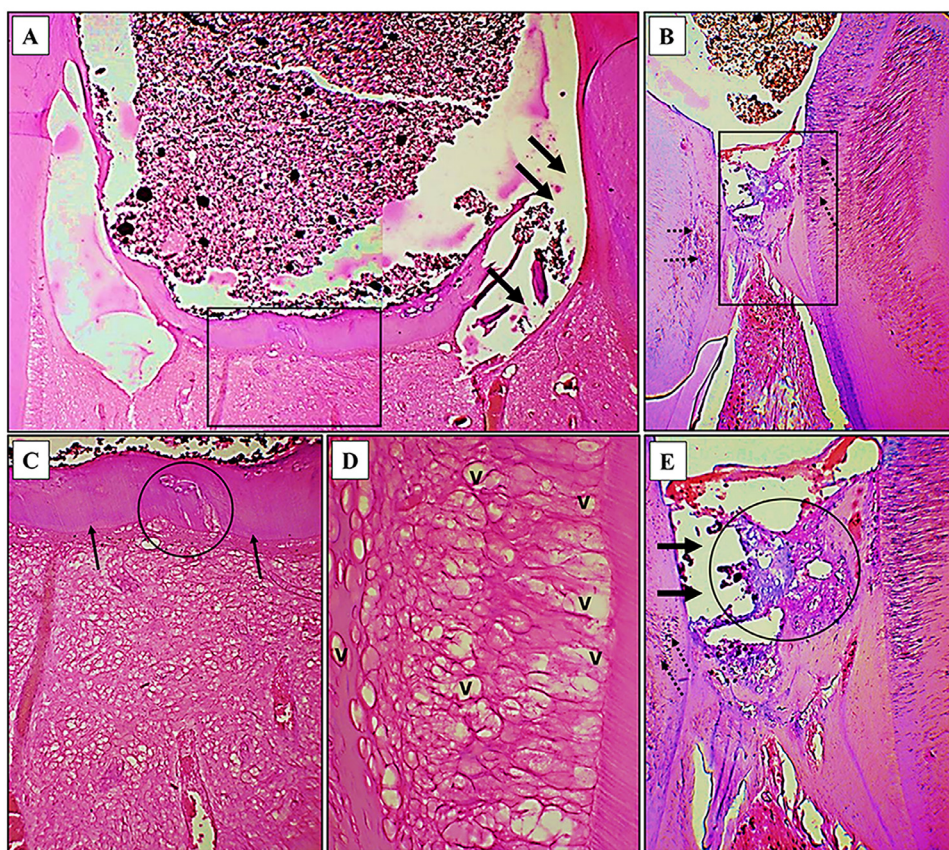


Figure 7 – Decalcified sections (DSs), H&E, subgroup III2 (MTA) (8 weeks). A-C and E show two calcified bridges. A is a compound figure. C and E are higher magnifications of the boxed areas in A and B, respectively. D is a higher magnification of an area from a deeper section of that seen in C. In A-C and E the formed bridges are non-homogeneous showing moderate thickness, variable organisation, containing defective structures (circles) and lack of complete attachment to dentin walls (thick arrows). In C note the tubular dentin-like structure of the formed bridge, the thin layer of pre-dentin-like tissue and adjacent disorganised odontoblasts (thin arrows). MTA particles are seen incorporated into the formed bridges (A, B, C and E), inside the native dentin (dotted arrows in B and E) and in adjacent pulp tissue (A, B, C and E). In C and D note the complete disorganisation of the pulp tissue with many small vacuoles (v) between the odontoblasts and in deeper pulp tissue. Magnification: A (compound figure) and B— $\times 100$; C-E— $\times 400$.

the root canals and attached to dentin walls on both sides (Figures S6 and S7A-F and Tables S5 and S6, supplementary data). Consequently, this might be a pointer to the quick promising pulpal response to both the applied alginate/BMBG NPs loaded hydrogel and pulpotomy procedure.

In the case of FD bridges, various studies reported that fibrodentin usually prefaced the production of mature tubular dentin because it constituted fibronectin, osteopontin (OPN) and bone sialoprotein (BSP) (noncollagenous proteins). These proteins are mandatory for the mineralisation mechanism. In addition, they play a major role in the migration of progenitor cells and their differentiation into odontoblast-like cells.⁴⁷

Regarding OD bridges, the appearance of connective tissue with multiple cellular inclusions and the absence of a tubular configuration might indicate the rapid attempt to provide a “protective barrier” of a sealing effect to the underlying pulp tissue.⁴¹ Furthermore, it can be assumed that this early atubular dentin could be sequentially incorporated with dentinal tubule-like structures as soon as mineralisation proceeds.

Also, it could suggest the incomplete differentiation of mesenchymal cells into odontoblast-like cells.

Extraordinarily, dentin-like tissue deposits were obviously noted inside the hydrogel pores. This could be considered as a powerful indication of the conductive/inductive behaviour of the applied novel hydrogel for reparative dentin formation, acting as a template onto which progenitor cells attach and begin the differentiation process into odontoblast-like cells for reparative dentinogenesis (Figure S11, supplementary data). Additionally, alginate, because of its temperature-independent gel condition and existence of multivalent cations, was appropriate for cell immobilisation, thus protecting them from any stress as they were physically confined.⁴⁸

Another remarkable feature was noticed where the boron nanoparticles were homogeneously filling the hydrogel pores. Consequently, this could indicate that boron ions were successfully liberated from BMBG NPs upon degradation and began to share in the reparative dentinogenesis alongside other released ions such as calcium, phosphorus, silicon, and

so on. Subsequently, all those liberated ions might have tended to chemically guide (chemotaxis) progenitors to the mineralisation route (Figure S11, supplementary data).

Furthermore, various structures of the newly created dentin bridges were traced after 4 weeks, yet most of them were of higher moderate thickness than those of the 2 weeks, although the difference was statistically significant. In addition, 1 of these bridges displayed a homogenous, tubular pattern accompanied by odontoblast-like cells arranged on its apical border. This may denote the impact of odontoblast-like cells alignment on their function and consequent production of the dentin matrix. Notably, a regenerated dentin (rd) layer was observed lining both sides of the root canal. Moreover, traces of hydrogel were observed in the superficial border of the formed bridge, which could suggest the hydrogel transformation into a dentin bridge because it is a bioresorbable biomaterial, recently considered to be part of a bioactivity process.⁴⁹ The brownish colour of boron nanoparticles was clearly seen within the formed dentin bridges, which could strongly emphasise the sustained release of boron ions after 4 weeks and its strong participation in dentin regeneration (Figure S11, supplementary data).

Consistent with other studies,⁵⁰ another outstanding feature traced in hydrogel group after 4 weeks was 1 of the bridges (ectopic dentin bridge [edb]) forming away from the exposure site. Interestingly, that edb bridge was homogenous, continuous, of moderate thickness and exhibited tubular configurations. Moreover, this edb merged with the rd that was formed along the adjacent canal wall. This might suggest the powerful distant regenerative (inductive) effect of the applied hydrogel through the effective diffusion of the released ions (calcium, phosphorus, silicon, and boron ions). The diffused ions into deeper parts of the pulp tissue could have attracted various types of undifferentiated mesenchymal stem cells present in human dental tissue (Figure S11, supplementary data).

Interestingly, after 8 weeks, all teeth in the hydrogel group exhibited the thickest and regular dentin bridge formation, which was statistically significant ($P \leq .05$) (Figure 4, Figure S6, and Tables S5 and S6, supplementary data). Distinctly, 2 forms of dentin-like tissue deposition (regenerated dentin (rd) and dentin bridge [db]) were clearly distinguished, very comparable to those seen at 4 weeks. Basically, these 2 regenerative variants were structurally quite like each other but were far different from the original native dentin. This could be explained by the absence of traditional signalling from ameloblasts and their membranes.⁵¹ Importantly, it is essential to differentiate between these 2 newly formed dentin-like tissues and not to consider them as 1 type because the mechanism of their production is different. They are different in their location and histological structure. Regenerated dentin (rd) was deposited on top of the pre-existing dentin of the root canal walls, and this allowed odontoblast-like cells to extend their processes into already existing dentinal tubules, while the dentin bridge (db) was deposited underneath the applied hydrogel which acted as a template (conductive effect) onto which progenitor cells adhered and differentiated into odontoblast-like cells. Later on, these differentiated cells lay down dentin-like tissue and then drag behind their processes for dentinal tubules to be created.⁵¹

In compliance with previous studies, the development of regenerated dentin (rd) along root canal walls could be an outcome of two prospects. One perspective is that this may be a result of the inductive environment created by the applied novel hydrogel for the growth, migration, adhesion, and differentiation of pulpal cells. This inductive effect might be brought about by the release of bioactive molecules (dentin matrix proteins) such as growth factors, cytokines, neuropeptides, glycosaminoglycans and plasma proteins, among others, from pre-existing undamaged dentin in response to ion dissolution from the applied hydrogel (Figure S11, supplementary data). These molecules could promote reparative dentinogenesis given that they have been shown to participate in the mineralisation process and serve as signalling molecules involved in the differentiation of odontoblast progenitors.⁵²

According to the other perspective, many researchers declared deposition of multiple layers of reparative dentin along root canal walls which presented as reparative dentin with a disorganised, irregular tubular pattern or as entrapped cells in the cytoplasm devoid of tubular structures, very similar to osteoid tissue (osteodentin).⁵³ They attributed these histological alterations that happened in radicular dentin to 'fibro proliferative reaction'^{54,55} of fibroblasts because they proved to proliferate more rapidly than stem progenitor cells.⁵³ Similarly, another study explored two different forms of dentin-like tissue deposits in the same tooth, in response to inflammatory reaction after pulp capping with Biodentin in rats.⁵⁶ They attributed this outcome to the uncertainty of pulp state under deep carious lesions and bacterial contamination. In fact, after a destructive carious attack, odontoblasts are damaged. Sequentially, cells present in the subodontoblastic zone would differentiate, inducing mineralisation at the pulp tissue boundary by forming the so-called reactionary dentin.⁵⁶

Therefore, the development of both regenerative variants (rd and db) after 8 weeks might be considered as a sign of successful conductive /inductive regenerative effect of the applied novel hydrogel, which provided a suitable microenvironment for adequate differentiation of progenitors into functional odontoblast-like cells (Figure S11, supplementary data). These odontoblast-like cells regenerated functional tubular dentin, which provided mechanical resilience to the tooth and participated in tooth sensitivity and immune response.⁵²

Of note, this outstanding dentin regenerative state could be attributed to various factors. Some might be related to alginate as a natural component of hydrogel, while others might be related to BMBG NPs as a synthetic component (in organic bioactive nanofiller) of the novel hydrogel (Figures S10 and S11, supplementary data). Basically, alginate has many advantages, previously discussed, that support its use as a scaffold in the regenerative field.

Next, BMBG NPs exhibited several characteristics which could empower their role in dentin regeneration. Importantly, BMBG NPs are highly bioactive and their addition increased the precipitation of carbonated hydroxyapatite crystals on scaffolds surface^{14,15} (Figures S10 and S11, supplementary data). Furthermore, this bone-like apatite layer facilitated a direct bond between the applied hydrogel and human

cells (progenitor cells).¹⁴ In regard to various studies in literature, bioactive glass-based scaffolds upregulate the expression of various growth factors such as bone morphogenetic proteins (BMP-2, BMP-4, BMP-7),⁵⁷ which are considered among the most fundamental factors of dentin regeneration.

Also, nano-topography of BMBG NPs (particle size ~ 50 nm), which is close to histological apatite created in human dentin,⁵⁸ and the spherical particle shape both promoted dentin regeneration. This was achieved by a collaborative behaviour of cell migration, surface adhesion, polarisation, cell differentiation and mineralisation. This was in agreement with Wang et al.,⁵⁹ who found a significant increase in different odontogenic associated genes and proteins (collagen type I, dentin sialo phosphoprotein and dentin matrix protein 1) of human dental pulp cells (hDPCs) in n BG group compared to control group.⁵⁹ Besides, surface characteristics of BMBG NPs such as hydrophilicity and surface charge would further promote cell adhesion. This is in accordance with Lee et al.,⁶⁰ who found that, in rat dental pulp cells, nBG elevated the expression of different odontogenic associated genes and mineralisation potential.⁶⁰

Additionally, the presence of boron played an active role in promoting reparative dentinogenesis. This was consistent with Moonesi et al.,¹⁴ who declared that boron-doped BG favourably influenced BG bioactivity, odontogenic differentiation of hDPSCs, and cell viability.¹⁴

Based on the outcomes of the current study and our previous work,¹⁵ it could be suggested that the innovative injectable alginate/BMBG NPs (20 wt. %) loaded hydrogel could act as a transportation vehicle. Also, the addition of boron-doped mesoporous bioactive glass nanoparticles (20 wt. %) attenuated the unfavourable consequences of sodium alginate. It enhanced porosity and pore size and increased water absorption. Moreover, it showed a powerful bioactive capacity and cell viability¹⁵ (Figure S10, supplementary data). Along the same lines, Osorio et al.⁶¹ reported that the incorporation of tideglusib-doped nanoparticles (TDg-NPs) reduced the unpleasant sequelae of lipopolysaccharide (LPS), thus enhancing regenerative mineralisation and osteogenic capacity of human dental pulp stem cells (hDPSCs) in the regenerative field.⁶¹ Along similar lines, López-García et al.⁶² indicated that the addition of graphene oxide (GO), silk fibroin (SF) and reduced graphene oxide (rGO) in appropriate compositions and structure decreased the drawbacks associated with cell (hDPSCs) proliferation and differentiation.⁶²

Although MTA was regarded as the gold standard for vital pulp treatment approaches, it exhibited a less favourable performance as a pulpotomy filling material compared to the newly applied hydrogel in terms of dentin bridge thickness, continuity and quality. This was statistically significant ($P \leq .05$) over 4 weeks and 8 weeks (Figures 6 and 7, Figure S6, and Tables S5 and S6, supplementary data).

Remarkably, after 2 weeks, different forms of dentin bridges were traced in the MTA group. In general, most of them exhibited mild thickness and were attached to both dentin walls of the root canal. After 4 weeks, a relatively greater number of teeth with dentin bridges of moderate thickness were displayed compared to 2 weeks, with no statistical significance. Moreover, most of these bridges were disorganised, showing obvious layers of fibrodentin and osteodentin.

Of note, after 8 weeks, despite the presence of a large number of teeth exhibiting newly formed bridges of moderate thickness, most of these bridges were not homogenous. Moreover, they contained defective structures with lack of actual attachment to the dentin walls of the root canal. Also, MTA particles were evidently seen in the formed bridges, inside the native dentin and in adjacent pulp tissue. Complete disorganisation, vacuolation and disarranged odontoblast-like cells were displayed in the adjacent pulp. This leads to a conclusion that although a dentin bridge was formed, it was not efficient enough to protect the underlying radicular pulp tissue from an external attack. Furthermore, the inferior pulpal response could emphasise the poor biocompatibility of MTA.

Collectively, this negative performance of MTA agrees with various results reported in the literature. Accorinte et al.⁶³ found retarded dentin bridge formation after 30 days in MTA (Angelus) group in relation to calcium hydroxide powder protected by a layer of calcium hydroxide cement on top. This comparative study accredited this outcome to both the high alkalinity of calcium hydroxide (pH 11 to 13) compared to MTA (pH 10) and to the stronger antimicrobial characteristic of calcium hydroxide powder in relation to MTA.⁶³ Additionally, various reported studies related this poor performance of MTA to the dissolution of calcium hydroxide and other hydration outcomes from MTA which deleteriously affect some of its physical characteristics, including inadequate adaptation and microleakage and great porosity.⁶⁴ Similarly, Dammaschke et al.⁶⁵ noticed a disordered, non-homogenous dentin bridge which lacked tubular configuration and showed many tunnel defects following pulp capping of human teeth with Retro MTA. They attributed this observation to the hydrophilic nature of Retro MTA which might affect the pulpal response, as well as to the operative obstacles that were experienced during the study.⁶⁵

In the present study, the alginate/BMBG NPs (20 wt. %) loaded injectable hydrogel has shown promise for improving inflammatory cell response, maintaining pulp vitality and regenerating dentin as an alternative to MTA. As with all studies, some limitations were experienced in the present work. The first 1 concerns the method used for histological evaluation which relies on a scoring system (quantitative analysis).²⁵ A quantitative analysis of the histological parameters such as total surface area, formation rate, and compactness is more reliable than inflammatory cell count⁶⁶ and reparative dentin bridge formation (histomorphometrical analysis).^{67,68} A relatively sample size is another limitation which should be overcome in future research. Furthermore, this study was performed on sound, caries-free teeth, but in the clinical environment, it is the carious teeth that go through pulpotomy. Immunohistochemistry could be performed to show immunomarkers such as OPN and osteocalcin to sustain dentin bridge formation. Another notable outcome of the current study was the leakage of tested pulpotomy filling materials into the pulp of some specimens. This can be a result of the application approach or material composition. The pulpotomy agents should be administered cautiously, without any condensation, on top of the remaining pulp tissue. Escape of material into the pulp might reduce the rate of healing and affect dentin bridge

formation.⁶⁹ Furthermore, extended observational periods could be used. Further research is needed to apply the novel injectable alginate/BMBG NPs loaded hydrogel in clinical trials.

Conclusions

Sodium alginate/BMBG NPs (20 wt.%), a nanoparticle-polymer-based hydrogel, made headway as a regenerative pulpotomy filling biomaterial possessing safe biocompatibility and conductive/inductive potential for monitoring dentinogenesis. Consequently, it might perform as a promising substitute for MTA in regenerative pulpotomy. Further long-term *in vivo* studies and potential clinical applications are needed to be conducted.

Author contributions

Analysis: Kamoun, Naga

Conceptualisation: El Din, Ghareeb, Kamoun, Moaty, Naga, Omar

Data collection: Kamoun, Naga

Data curation: Ghareeb, Moaty, Omar

Design: El Din, Ghareeb, Kamoun, Moaty, Naga, Omar

Investigation: Ghareeb, Moaty, Omar

Material arrangement: Kamoun, Naga

Methodology: Ghareeb, Moaty, Omar

Study design: El Din, Kamoun

Visualisation: Ghareeb, Moaty, Omar

Writing – original draft: Ghareeb, Kamoun, Moaty, Naga, Omar

Writing – review and editing: El Din, Ghareeb, Kamoun, Moaty, Naga, Omar

Funding statement

This research did not receive any specific grant from funding agencies in the public, commercial, or not-for-profit sectors.

Conflict of interest

The authors declare no conflict of interests.

Supplementary materials

Supplementary material associated with this article can be found in the online version at doi:10.1016/j.identj.2025.04.008.

REFERENCES

- Zhang L, Yin L, Wu J, Wang X, Huang J, Li Q. Clinical influencing factors of vital pulp therapy on pulpitis permanent teeth with 2 calcium silicate-based materials: a randomized clinical trial. *Medicine (Baltimore)* 2024;103:e38015. doi: 10.1097/md.00000000000038015.
- Bjørndal L, Simon S, Tomson PL, Duncan HF. Management of deep caries and the exposed pulp. *Int Endod J* 2019;52:949–73. doi: 10.1111/iej.13128.
- World Health Organization (WHO). Oral health. Geneva: WHO. 2025. Available from: <https://www.who.int/news-room/fact-sheets/detail/oral-health>. Accessed 20 March 2025.
- Sequeira DB, Diogo P, Gomes B, Peça J, Santos JMM. Scaffolds for dentin-pulp complex regeneration. *Medicina (Kaunas)* 2023;60:7. doi: 10.3390/medicina60010007.
- Haugen HJ, Basu P, Sukul M, Mano JF, Reseland JE. Injectable biomaterials for dental tissue regeneration. *Int J Mol Sci* 2020;21:3442. doi: 10.3390/ijms21103442.
- Farshidfar N, Iravani S, Varma RS. Alginate-based biomaterials in tissue engineering and regenerative medicine. *Mar Drugs* 2023;21:189. doi: 10.3390/md21030189.
- Kaou MH, Furkó M, Balázs K, Balázs C. Advanced bioactive glasses: the newest achievements and breakthroughs in the area. *Nanomaterials (Basel)* 2023;13:2287. doi: 10.3390/nano13162287.
- Anand A, Kaňková H, Hájovská Z, Galusek D, Boccaccini AR, Galusková D. Bio-response of copper-magnesium co-substituted mesoporous bioactive glass for bone tissue regeneration. *J Mater Chem B* 2024;12:1875–91. doi: 10.1039/d3tb01568h.
- Xie H, Sha S, Lu L, et al. Cerium-containing bioactive glasses promote *in vitro* lymphangiogenesis. *Pharmaceutics* 2022;14:225. doi: 10.3390/pharmaceutics14020225.
- Al-Harbi N, Mohammed H, Al-Hadeethi Y, et al. Silica-based bioactive glasses and their applications in hard tissue regeneration: a review. *Pharmaceutics (Basel)* 2021;14:75. doi: 10.3390/ph14020075.
- Warington K. The effect of boric acid and borax on the broad bean and certain other plants. *Ann Bot* 1923;37:629–72.
- Balasubramanian P, Büttner T, Pacheco VM, Boccaccini AR. Boron-containing bioactive glasses in bone and soft tissue engineering. *J Eur Ceram Soc* 2018;38:855–69.
- Gharbi A, Oudadesse H, El Feki H, et al. High boron content enhances bioactive glass biodegradation. *J Funct Biomater* 2023;14:364.
- Moonesi Rad R, Pazarçeviren E, Ece Akgün E, et al. *In vitro* performance of a nanobiocomposite scaffold containing boron-modified bioactive glass nanoparticles for dentin regeneration. *J Biomater Appl* 2019;33:834–53. doi: 10.1177/0885328218812487.
- Naga MS, Helal HM, Kamoun EA, et al. A novel injectable boron doped-mesoporous nano bioactive glass loaded-alginate composite hydrogel as a pulpotomy filling biomaterial for dentin regeneration. *BMC Oral Health* 2024;24:1087.
- Negm AM, Hassanien EE, Abu-Seida AM, Nagy MM. Biological evaluation of a new pulp capping material developed from Portland cement. *Exp Toxicol Pathol* 2017;69:115–22. doi: 10.1016/j.etp.2016.12.006.
- Petrie A, Sabin C. *Medical statistics at a glance*. 3rd ed. West Sussex: John Wiley & Sons; 2009.
- Holiel AA, Mahmoud EM, Abdel-Fattah WM, Kawana KY. Histological evaluation of the regenerative potential of a novel treated dentin matrix hydrogel in direct pulp capping. *Clin Oral Investig* 2021;25:2101–12. doi: 10.1007/s00784-020-03521-z.
- Al-Sherbiny IM, Abu-Seida AM, Farid MH, Motawea IT, Bastawy HA. Histopathological pulp response of dog's teeth capped with biosealer and biodentine: an *in vivo* study. *Saudi Endod J* 2020;10:226–33.
- Sedek EM, Abdelkader S, Fahmy AE, Kamoun EA, Nouh SR, Khalil NM. Histological evaluation of the regenerative potential of a novel photocrosslinkable gelatin-treated dentin matrix hydrogel in direct pulp capping: an animal study. *BMC Oral Health* 2024;24:114. doi: 10.1186/s12903-024-03868-9.
- Singh J. Randomization and online databases for clinical trials. *J Pharmacol Pharmacother* 2014;5:173–4. doi: 10.4103/0976-500x.130155.

22. Schulz KF. Allocation concealment. In: D'Agostino RB, Sullivan LM, Massaro JM, editors. *Wiley encyclopedia of clinical trials*. Hoboken, NJ: Wiley; 2007. p. 2524.
23. Metwally NI, RM EA, Ahmed NA, Zaghloul SA. Histologic comparison of formocresol, platelet-rich fibrin, and hesperidin in pulpotomy: a randomized trial in dogs. *Niger J Clin Pract* 2023;26:856–62. doi: [10.4103/njcp.njcp_1731_21](https://doi.org/10.4103/njcp.njcp_1731_21).
24. Sayed MM, Khattab N, Ahmed W. Histopathological and histochemical evaluation of pulpal response to biodentine compared to Portland cement in pulpotomized dogs' teeth. *EC Dent Sci* 2018;17:261–72.
25. Nowicka A, Parafiniuk M, Lipski M, Lichota D, Buczkowska-Radlinska J. Pulpo-dentin complex response after direct capping with self-etch adhesive systems. *Folia Histochem Cyto-biol* 2012;50:565–73. doi: [10.5603/20325](https://doi.org/10.5603/20325).
26. McDonald RE, Avery DR, Jeffrey AD. Treatment of deep caries, vital pulp exposure, and pulp less teeth. In: McDonald RE, Avery DR, editors. *Dentistry for the child and adolescent*. 9th ed Missouri: Mosby, Elsevier; 2011. p. 350.
27. Taha NA, Abdelkhalder SZ. Outcome of full pulpotomy using biodentine in adult patients with symptoms indicative of irreversible pulpitis. *Int Endod J* 2018;51:819–28. doi: [10.1111/iej.12903](https://doi.org/10.1111/iej.12903).
28. Abo El-Mal EO, Abu-Seida AM, El Ashry SH. Biological evaluation of hesperidin for direct pulp capping in dogs' teeth. *Int J Exp Pathol* 2021;102:32–44. doi: [10.1111/iej.12385](https://doi.org/10.1111/iej.12385).
29. Tao S, Yang T, Zhou JN, Zhang Q. Impaired pulp healing associated with underlying disorders in the dental pulp of rats with type 2 diabetes. *J Dent Sci* 2024;19:310–20. doi: [10.1016/j.jds.2023.03.021](https://doi.org/10.1016/j.jds.2023.03.021).
30. Al-Saudi KW, Nabih SM, Farghaly AM, AboHager EA. Pulpal repair after direct pulp capping with new bioceramic materials: a comparative histological study. *Saudi Dent J* 2019;31:469–75. doi: [10.1016/j.sdentj.2019.05.003](https://doi.org/10.1016/j.sdentj.2019.05.003).
31. Shah A. Evaluation of pulpal and dentin regeneration by different pulp-capping materials using mouse model. (Doctoral dissertation, UCLA); 2019.
32. Hallab NJ, Jacobs JJ. Biologic effects of implant debris. *Bull NYU Hosp Jt Dis* 2009;67:182–8.
33. Naseri S, Lepry WC, Nazhat SN. Bioactive glasses in wound healing: hope or hype? *J Mater Chem B* 2017;5:6167–74. doi: [10.1039/c7tb01221g](https://doi.org/10.1039/c7tb01221g).
34. Brown RF, Rahaman MN, Dwilewicz AB, et al. Effect of borate glass composition on its conversion to hydroxyapatite and on the proliferation of MC3T3-E1 cells. *J Biomed Mater Res A* 2009;88:392–400. doi: [10.1002/jbm.a.31679](https://doi.org/10.1002/jbm.a.31679).
35. Munukka E, Leppäranta O, Korkeamäki M, et al. Bactericidal effects of bioactive glasses on clinically important aerobic bacteria. *J Mater Sci Mater Med* 2008;19:27–32. doi: [10.1007/s10856-007-3143-1](https://doi.org/10.1007/s10856-007-3143-1).
36. Abd El Bary K, El Shafei JM, Roshdy NN. Comparison of the effect of calcium hydroxide nanoparticles paste versus double antibiotic paste used in regenerative endodontic procedure on the chemical structure of radicular dentin (an in vitro study). *Acta Sci Dent Sci* 2019;3:1–9.
37. Reyes-Carmona JF, Santos AR, Figueiredo CP, Felipe MS, Felipe WT, Cordeiro MM. In vivo host interactions with mineral trioxide aggregate and calcium hydroxide: inflammatory molecular signaling assessment. *J Endod* 2011;37:1225–35. doi: [10.1016/j.joen.2011.05.031](https://doi.org/10.1016/j.joen.2011.05.031).
38. Pintado-Palomino K, de Almeida C, da Motta RJG, Fortes JHP, Tirapelli C. Clinical, double blind, randomized controlled trial of experimental adhesive protocols in caries-affected dentin. *Clin Oral Investig* 2019;23:1855–64. doi: [10.1007/s00784-018-2615-7](https://doi.org/10.1007/s00784-018-2615-7).
39. Shayegan A, Petein M, Abbeele AV. Beta-tricalcium phosphate, white mineral trioxide aggregate, white Portland cement, ferric sulfate, and formocresol used as pulpotomy agents in primary pig teeth. *Oral Surg Oral Med Oral Pathol Oral Radiol Endod* 2008;105:536–42. doi: [10.1016/j.tripleo.2007.10.008](https://doi.org/10.1016/j.tripleo.2007.10.008).
40. Zheng K, Fan Y, Torre E, et al. Incorporation of boron in mesoporous bioactive glass nanoparticles reduces inflammatory response and delays osteogenic differentiation. *Part Part Syst Charact* 2020;37:2000054.
41. Arafa HA, Niazy MA, Eissa M, Elmoaty MA. Histopathological changes after direct pulp capping in dogs with bioactive glass incorporated in resin composite and adhesive. *Al-Azhar Dent J Girls* 2021;8:535–52.
42. Bakhtiar H, Aminishakib P, Ellini MR, et al. Dental pulp response to RetroMTA after partial pulpotomy in permanent human teeth. *J Endod* 2018;44:1692–6. doi: [10.1016/j.joen.2018.07.013](https://doi.org/10.1016/j.joen.2018.07.013).
43. Tang JJ, Shen ZS, Qin W, Lin Z. A comparison of the sealing abilities between Biodentine and MTA as root-end filling materials and their effects on bone healing in dogs after periradicular surgery. *J Appl Oral Sci* 2019;27:e20180693. doi: [10.1590/1678-7757-2018-0693](https://doi.org/10.1590/1678-7757-2018-0693).
44. Mostafa NM, Moussa SA. Mineral trioxide aggregate (MTA) vs calcium hydroxide in direct pulp capping: literature review. *ARC J Dent Sci* 2018;3:18–25.
45. Balto HA. Attachment and morphological behavior of human periodontal ligament fibroblasts to mineral trioxide aggregate: a scanning electron microscope study. *J Endod* 2004;30:25–9. doi: [10.1097/00004770-200401000-00005](https://doi.org/10.1097/00004770-200401000-00005).
46. Schembri M, Peplow G, Camilleri J. Analyses of heavy metals in mineral trioxide aggregate and Portland cement. *J Endod* 2010;36:1210–5. doi: [10.1016/j.joen.2010.02.011](https://doi.org/10.1016/j.joen.2010.02.011).
47. Kuratate M, Yoshida K, Shigetani Y, Yoshida N, Ohshima H, Okiji T. Immunohistochemical analysis of nestin, osteopontin, and proliferating cells in the reparative process of exposed dental pulp capped with mineral trioxide aggregate. *J Endod* 2008;34:970–4. doi: [10.1016/j.joen.2008.03.021](https://doi.org/10.1016/j.joen.2008.03.021).
48. Sequeira DB, Diogo P, Gomes BP, Peça J, Santos JMM. Scaffolds for dentin–pulp complex regeneration. *Medicina* 2023;60:7.
49. Wheeler DL, Stokes KE, Hoellrich RG, Chamberland DL, McLoughlin SW. Effect of bioactive glass particle size on osseous regeneration. *J Biomed Mater Res* 1999;46:301–3.
50. Jose B, Ratnakumari N, Mohanty M, Varma HK, Komath M. Calcium phosphate cement as an alternative for formocresol in primary teeth pulp potomies. *Indian J Dent Res* 2013;24:522. doi: [10.4103/0970-9290.118370](https://doi.org/10.4103/0970-9290.118370).
51. Huang GT, Garcia-Godoy F. Missing concepts in de novo pulp regeneration. *J Dent Res* 2014;93:717–24. doi: [10.1177/0022034514537829](https://doi.org/10.1177/0022034514537829).
52. Lee M, Lee YS, Shon WJ, Park JC. Physiologic dentin regeneration: its past, present, and future perspectives. *Front Physiol* 2023;14:1313927. doi: [10.3389/fphys.2023.1313927](https://doi.org/10.3389/fphys.2023.1313927).
53. Ricucci D, Loghin S, Lin LM, Spångberg LS, Tay FR. Is hard tissue formation in the dental pulp after the death of the primary odontoblasts a regenerative or a reparative process? *J Dent* 2014;42:1156–70. doi: [10.1016/j.jdent.2014.06.012](https://doi.org/10.1016/j.jdent.2014.06.012).
54. Álvarez-Vásquez JL, Castañeda-Alvarado CP. Dental Pulp Fibroblast: A Star Cell. *J Endod* 2022;48:1005–19. doi: [10.1016/j.joen.2022.05.004](https://doi.org/10.1016/j.joen.2022.05.004).
55. Boraldi F, Lofaro FD, Bonacorsi S, Mazzilli A, Garcia-Fernandez M, Quaglino D. The Role of Fibroblasts in Skin Homeostasis and Repair. *Biomedicines* 2024;12:1586. doi: [10.3390/biomedicines12071586](https://doi.org/10.3390/biomedicines12071586).
56. Goldberg M, Njeh A, Uzunoglu E. Is pulp inflammation a prerequisite for pulp healing and regeneration? *Mediat Inflamm* 2015;2015:347649.
57. Eriksson E, Björkenheim R, Strömberg G, et al. S53P4 bioactive glass scaffolds induce BMP expression and integrative bone formation in a critical-sized diaphysis defect treated with a single-staged induced membrane technique. *Acta Biomater* 2021;126:463–76. doi: [10.1016/j.actbio.2021.03.035](https://doi.org/10.1016/j.actbio.2021.03.035).

58. Hussain SS. Evaluation of pulpal and dentin regeneration by different pulp-capping materials using mouse model. MSc thesis, 2019.
59. Wang S, Gao X, Gong W, Zhang Z, Chen X, Dong Y. Odontogenic differentiation and dentin formation of dental pulp cells under nanobioactive glass induction. *Acta Biomater* 2014;10:2792–803. doi: [10.1016/j.actbio.2014.02.013](https://doi.org/10.1016/j.actbio.2014.02.013).
60. Lee JH, Kang MS, Mahapatra C, Kim HW. Effect of aminated mesoporous bioactive glass nanoparticles on the differentiation of dental pulp stem cells. *PLoS One* 2016;11:e0150727. doi: [10.1371/journal.pone.0150727](https://doi.org/10.1371/journal.pone.0150727).
61. Osorio R, Rodríguez-Lozano FJ, Toledano M, et al. Mitigating lipopolysaccharide-induced impairment in human dental pulp stem cells with tideglusib-doped nanoparticles: enhancing osteogenic differentiation and mineralization. *Dent Mater* 2024;40:1591–601. doi: [10.1016/j.dental.2024.07.012](https://doi.org/10.1016/j.dental.2024.07.012).
62. López-García S, Aznar-Cervantes SD, Pagán A, et al. 3D graphene/silk fibroin scaffolds enhance dental pulp stem cell osteo/odontogenic differentiation. *Dent Mater* 2024;40:431–40. doi: [10.1016/j.dental.2023.12.009](https://doi.org/10.1016/j.dental.2023.12.009).
63. Accorinte ML, Loguerio AD, Reis A, et al. Response of human dental pulp capped with MTA and calcium hydroxide powder. *Oper Dent* 2008;33:488–95. doi: [10.2341/07-143](https://doi.org/10.2341/07-143).
64. Kuratate M, Shigetani Y, Han L, Okiji T. Compositional change of mineral trioxide aggregate immersed in water: alteration of elemental distribution in the surface layer. *Japanese J Conserv Dent* 2009;52:348–54.
65. Dammaschke T, Nowicka A, Lipski M, Ricucci D. Histological evaluation of hard tissue formation after direct pulp capping with a fast-setting mineral trioxide aggregate (RetroMTA) in humans. *Clin Oral Investig* 2019;23:4289–99. doi: [10.1007/s00784-019-02876-2](https://doi.org/10.1007/s00784-019-02876-2).
66. Tawfik H, Abu-Seida AM, Hashem AA, Nagy MM. Regenerative potential following revascularization of immature permanent teeth with necrotic pulps. *Int Endod J* 2013;46:910–22. doi: [10.1111/iej.12079](https://doi.org/10.1111/iej.12079).
67. Hayashi K, Handa K, Koike T, Saito T. The possibility of genistein as a new direct pulp capping agent. *Dent Mater J* 2013;32:976–85. doi: [10.4012/dmj.2013-091](https://doi.org/10.4012/dmj.2013-091).
68. Koike T, Polan MA, Izumikawa M, Saito T. Induction of reparative dentin formation on exposed dental pulp by dentin phosphoryn/collagen composite. *Biomed Res Int* 2014;2014:745139. doi: [10.1155/2014/745139](https://doi.org/10.1155/2014/745139).
69. Dominguez MS, Witherspoon DE, Gutmann JL, Opperman LA. Histological and scanning electron microscopy assessment of various vital pulp-therapy materials. *J Endod* 2003;29:324–33. doi: [10.1097/00004770-200305000-00003](https://doi.org/10.1097/00004770-200305000-00003).